Experimental investigation of the mechanical robustness of a commercial module and membrane-printed functional layers for flexible organic solar cells

Zhengyu Fan[a,*], Michele De Bastiani[b], Michele Garbugli[b], Carol Monticelli[a], Alessandra Zanelli[a], Mario Caironi[b]

[a] Architecture, Built Environment and Construction Engineering Department, Politecnico di Milano, Via Bonardi 9, 20133 Milan, Italy
[b] Center for Nano Science and Technology @PoliMi, Istituto Italiano di Tecnologia, Via Pascoli 70/3, 20133 Milan, Italy

A coupled mechanical and electrical characterization method to monitor the correlation of organic photovoltaic (OPV) electrode resistance and cell performance upon tensile strain and to verify the cause of deterioration and the effect of OPV performance under tensile stress has been developed. Both a commercial OPV module and ethylene tetrafluoroethylene (ETFE) membrane-printed OPV electrode layers have been tested by applying the method. The encapsulation layer strength has been found to be the mechanical bottleneck of the tested com-mercial OPV module. The decrease in the transparent electrode conductance has been found to be responsible for cell degradation upon tensile strain, with the threshold tensile strain at approximately 2%. A test results com-parison between ETFE- and polyethylene terephthalate (PET)-printed OPV layers demonstrated that ETFE-printed electrodes are less brittle and sensitive to tensile strain owing to the network pattern response of ETFE-printed electrodes. In addition, the adoption of Ag/poly(3,4-ethylenedioxythiophene) (PEDOT) layering can improve the tensile strain threshold to almost double to maintaining 80% of the initial normalized layer con-ductance through the advantage of its "bridging effect". Collectively, our results provide valuable information and illustrate a promising future for architectural membrane printed OPV.

Keywords: Photovoltaic, Organic solar cell, Membrane, ETFE, Mechanical, Electrical, characterization

1. Introduction

Organic photovoltaics (OPV) is a promising alternative to established crystalline silicon-based photovoltaic technologies owing to its higher flexibility and lower capital cost investments [1–3]. In particular, the high solution processability of its active materials enables the adoption of mass printing methods to manufacture high volumes in an effective way.

However, almost all current research of flexible OPV is carried out on common plastic substrates (PET, PEN, etc.) with inferior performance for architectural integration. Existing commercial OPV modules also neglect the application requirements as building integrated photovoltaic (BIPV) elements. Both can highly hinder their future applications in buildings.

Meanwhile, novel membrane materials, especially ethylene tetrafluoroethylene (ETFE), enjoy higher popularity as substitutes for glass in the contemporary architecture context, thanks to their extraordinary lightness, high transparency and flexibility [4,5].

The research integration of both can therefore help with the commercial application and market development of OPV while enhancing the versatility of architectural membrane products. Nevertheless, the great potential of an architectural membrane as a novel OPV printing substrate, based on its high performance properties, has never been explored.

This survey first explores the feasibility and applicability of OPV in the flexible architectural membrane integration scenarios. Because the membrane, the applied printing substrate of flexible PV in mainstream membrane products/structures (tensioned, pneumatic), is subjected to tensile stress through the application, the primary consideration of this integration scenario therefore becomes the strength and photovoltaic performance of the OPV layer/module under stress.

This study devised a novel experimental methodology based on coupled electrical characterization and uniaxial tensile tests to examine the mechanical robustness and electrical manifestations of membrane-integrated OPV upon stress.

In this research, the performance of an existing commercial OPV

Received 25 May 2016;
Received in revised form 14 August 2016;
Accepted 3 April 2018
Available online 04 April 2018

* Corresponding author.
E-mail addresses: Zhengyu.fan@polimi.it (Z. Fan), Michele.debastiani@iit.it (M. De Bastiani), Michele.garbugli@iit.it (M. Garbugli), Carol.monticelli@polimi.it (C. Monticelli), Alessandra.zanelli@polimi.it (A. Zanelli), Mario.caironi@iit.it (M. Caironi).

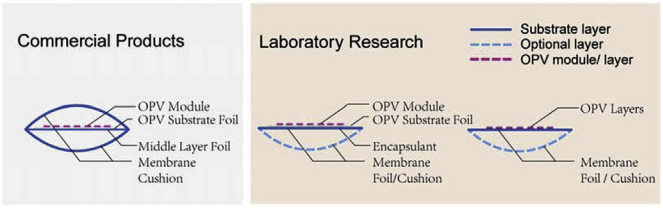

(a) (b) (c)

Fig. 1. Three strategies for membrane integrated flexible solar cells: (a) Mechanical integration; (b) Lamination; (c) Direct printing.

module under tensile stress is first reported to confirm its decay process and bottleneck limit of mechanical strength and electrical properties. Afterwards, this work uses the same method to examine the performance of functional OPV layers printed on an ETFE substrate under stress to explore the feasibility of architectural ETFE membrane-printed OPV layers, which can provide valuable knowledge for subsequent full OPV module printing on the ETFE membrane.

2. State of the art

Current OPV research has long focused on improving the power conversion efficiency and operational lifetime of the cell, whereas far less effort has been spent to optimize its integration for flexible building product development (and corresponding product performance).

Within the limited available research works concerning the OPV and even flexible PV integration onto/into architectural membrane foils/cushions, there are currently three main integration strategies (Fig. 1).

The first is to mechanically integrate flexible PV modules inside a cushion made of two or three membrane layers, with the edge fixed by either a mechanical or welding method (Fig. 1a). The embodied OPV module could be placed in either the upper or lower cavity.

An alternative process is to laminate the flexible PV module onto the membrane foil (Fig. 1b). This can be realized with suitable adhesive that can provide sufficient adhesion strength between the flexible PV module substrate and the membrane foil.

The most promising integration strategy is the direct printing of OPV modules onto the substrate foil, resulting in either single-layer membrane foil or integrated membrane cushion BIPV products (Fig. 1c).

All integration strategies require the incorporation of membrane substrate and functional OPV layers with distinct mechanical properties to form a composite product. Therefore, the mechanical properties of the OPV module and membrane, as well as their performance synergy, deserve investigation in detail. Meanwhile, the cell performance, with the functional layer in the condition of operational stress as integrated onto construction membranes, also must be verified. Both of the research topics lack relevant study.

To date, only limited work has been performed to understand the mechanical behaviour and electrical response under stress of OPV itself, and little has been reported about architectural membrane integrated OPV.

X. Chen and his co-workers investigated the mechanical behaviour of a commercially available OPV product from Konarka Technologies, Inc. through tensile testing [6,7]. With a uniaxial experiment, they obtained the nominal stress–strain curves for the full cell packaging and the individual layers, recorded the fracture sequence of each layer through the test, and showed that the two electrodes present in the stack are the short slab of the cell performance.

V. Brand et al. investigated the film stresses developed in polymer films and metal electrodes of P3HT and PCBM based bulk heterojunction organic solar cells [8]. They quantified the compressive stress in the PEDOT:PSS and Al electrode as well as the tensile stress in the BHJ layer. They also analysed the relationship between the deposition rate with the film stresses and cohesion among different layers. However, the effect of the stress on the layer and device performance has not been studied.

D. R. Cairns and his co-workers [9] noted the trade-off between thick layers of ITO to reduce resistivity and thin layers of ITO, which can withstand greater strain in the substrate.

Darren J. Lipomi and his group evaluated several different conjugated polymers with an effort to achieve a mechanically robust and intrinsically stretchable OPV [10–12]. They demonstrated the different responses upon tensile loads of poly(3,4-ethylenedioxythiophene):poly (styrenesulfonate) (PEDOT:PSS), poly-3-hexyl thiophene: phenyl-C61-butyric acid methyl ester (P3HT:PCBM), diketo pyrrolo-pyrrole moiety, thiophene, thienothiophene, and thiophene: phenyl-C61-butyric acid methyl ester (DPPT-TT:PCBM) fabricated on stretchable polydimethylsiloxane (PDMS) substrates. They also explored the crack and bulking effect through tensile tests, which are in favour of reversible stretchability. They have also investigated overall the stretchable, elastic and self-healing materials for OPV and electronic skins [13,14].

Toward the same endeavour, Kaltenbrunner, M et al. developed ultrathin and lightweight organic solar cells with high flexibility. They investigated the performance of their cells under extreme mechanical deformation and cyclic stretching tests. The performance of the tested solar cells was found to be able to withstand extreme mechanical deformations [15].

K. Leppanen et al. also studied the flexibility limit of ITO through bending tests [16]. The critical bending curvature and the correlation between the material conductivity and crack numbers were revealed.

However, the characterization of architectural membrane-printed OPV or its functional layers has not yet been started because no such cell structure has been fabricated. Even less work has been initialized with the mechanical flexibility of commercial polymer-printed OPV or its layers.

C. K. Cho, with his co-workers investigated the mechanical integrity of gravure printed PEDOT:PSS electrodes on the PET substrate through both bending and stretching tests [17]. They demonstrated that PEDOT:PSS film has superior stretchability relative to ITO electrodes. The same work group also tested the flexibility of a Ag nanowire (NW) network coated on a colourless polyimide CPI substrate peeled from a CPI/glass substrate sample [18]. The reported results also showed the higher flexibility of Ag NW over the ITO electrode. More recently, they tested the superior mechanical flexibility of transparent carbon nanotube (CNT) network electrodes prepared by a brush-painting method on PET for organic solar cells.

J. G. Tait et al. performed similar work to demonstrate that spray-coated PEDOT:PSS electrodes were able to withstand far greater mechanical deformation before failure than their ITO-based counterparts [19].

A. Iwan et al. further confirmed that ITO layers on PET foils are unsuitable for dynamic bending work conditions [20].

Meanwhile, S. Savagatrup et al. announced that P3HpT is an attractive potential replacement for P3HT in flexible, stretchable, and mechanically robust solar cells, as determined through tensile modulus comparison with P3HT and P3OT [21].

Some similar work has been performed with printed organic thin-film transistor (TFT)/light-emitting diodes (LEDs) or their electrode layers.

T. Sekine and his research group validated the adhesiveness importance of printed Ag electrodes on flexible plastic substrate for the mechanical durability and real performance of organic TFTs [22].

Z. Yu et al. developed and examined a highly stretchable electrode based on a carbon nanotube–polymer composite for their polymer light-emitting diodes [23]. The highly transparent electrode can be reversibly stretched by up to 50% strain with little change in sheet resistance.

Meanwhile, some research works have studied the performance response upon strain of amorphous silicon (a-si) solar cells and TFTs integrated on flexible substrates.

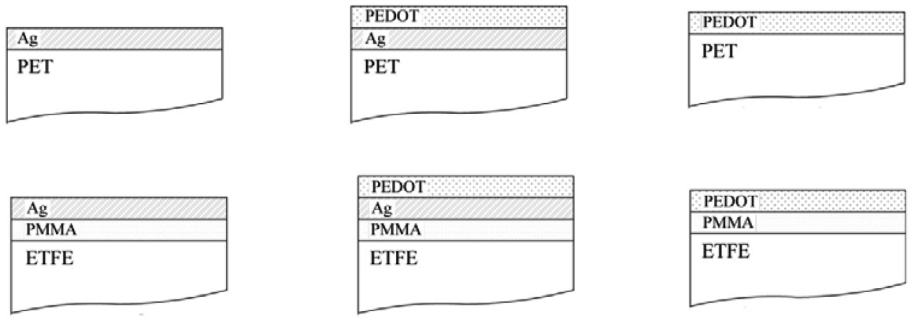

Fig. 2. Specimen layering structure.

R. Jones et al. defined the threshold values of curvatures and corresponding strains of both a-si solar cells and TFTs, employing the bending test [24]. They reported 0.75% as the strain limit for tension for a-si solar cells fabricated on 125 μm stainless steel substrate and 0.5% as the failure strain level for a-si TFTs while showing that compression up to 2% strain does not exert a strong effect on either.

H. Gleskova, S. Wagner and their co-workers reported the performance of a-si TFTs on Kapton and polymide foils [25–27]. They observed deteriorated electrical properties of TFTs on 25 μm Kapton after 2% compressive strain and 0.5% tensile strain through bending tests, along with a converse effect of tensile and compressive strain on TFTs fabricated on polyimide foil. They also found different responses between a-Si TFTs and solar cells to tensile strain. The threshold tensile strains of TFTs and solar cells have been defined as ~0.34% and ~0.7%, respectively.

D. Antartis and I. Chasiotis determined the residual stresses among different layers of a-Si photovoltaic thin films based on a Kapton layer and aluminium substrate (Antartis & Chasiotis, 2014). Residual stress in the Si and Si/ZnO layers were found to be significant, and the degradation of photovoltaics was found to occur at substrate strain higher than 0.8% [28].

Apart from sole stress effect on the mechanical behaviour of roll-to-roll(R2R) printed organic solar cells, the effect of other common stress factors such as high temperature, humidity and UV irradiation should also be considered. Only limited work have explored into this topic.

S. R. Dupont, R. H. Dauskardt and their coworkers have demonstrated that thermomechanical stresses can drive the loss of interlayer adhesion, and therefore the device performance of R2R processed inverted P3HT:PCBM bulk heterojunction polymer solar cells. They found that Post-Deposition annealing time and temperature can increase the adhesion at cell interface [29]. In a newer research the same work group reported that the combined application of different stress factors can strengthen the adhesion of certain OPV interfaces [30].

Considering the impact of both thermal and mechanical forces on R2R processed organic electronic devices, B. Roth, S. Savagatrup and their colleagues investigated the connection between molecular structures and polymer's mechanical properties. They found some general trends indication, which are useful for designing highly mechanically robust materials for R2R fabrication. They also pointed out the importance of co-optimization of electronic and mechanical properties for designing materials for both R2R fabrication and flexible or stretchable applications [31].

Here, we report the research outcome through a coupled electrical–mechanical test methodology to verify the effect of tension strain on the performance response of OPV. The test method enables real-time and simultaneous characterization of both mechanical and electrical properties of a tested flexible electronic composite. The experimental method can also monitor the correlation of OPV electrode resistance and cell performance upon tensile strain. A uniaxial tensile test has been utilized rather than a bending test because it is closer to the operational state of membrane integrated OPV products.

We employed this test methodology on both a commercial OPV module and its conductive layers printed on an architectural membrane. The test on the commercial OPV module can help elucidate the effectiveness of the first two integration strategies. The test on printed OPV layers on ETFE is even more appealing because the direct printing strategy is found to be the most promising production method of OPV. In absence of knowledge on membrane printed full OPV devices, preliminary research on the performance of printed OPV layers can already provide useful insights.

3. Experimental

The tested specimens were cut into dumbbell shaped specimens. Detailed specimen dimension can be checked in the section of supporting information.

For characterization of commercial OPV module, the specimens were fabricated from a commercial OPV product. For characterization of membrane printed OPV, the experiments have been performed on two types of electrode layers normally employed in OPV structure: Ag and Ag\PEDOT, printed on both PET and ETFE. The layering structures of different specimens are shown in Fig. 2. The thicknesses of different specimen layers and substrates are listed in Table 1.

The details of the coupled Mechanical and Electrical characterization, including the mechanical tensile test setup as well as the electrical characterization experimental configuration, will be further explained in the supporting information section.

4. Results and discussion

4.1. Characterization of commercial OPV modules

4.1.1. Stability test results

The stability test results for an individual cell cut from the whole module are reported in Fig. 3. It can clearly be seen that after the cells are stored for 22 h in the ambient environment, the efficiency does not show a significant decrease. The cell maintained more than 90% of its initial efficiency after being stored for 22 h in an ambient environment. This fact proves that it is safe and reliable to perform the tensile test with electrical characterization for several hours in an ambient environment.

Table 1
Thicknesses of tested specimens.

Specimen layers/substrates	Thickness
PEDOT	~100 nm
Ag	~200 nm
PMMA	~500 nm
PET	~75 μm
ETFE	~100 μm

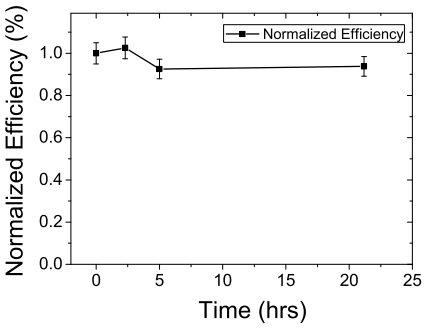

Fig. 3. Single-cell efficiency through stability test.

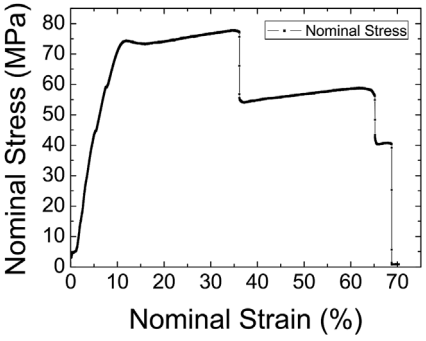

Fig. 4. Nominal stress–strain curve of full cell packaging.

4.1.2. Mechanical test results

Fig. 4 shows the nominal stress–strain curve of the tested OPV cell sample. Compared with the result reported by X. Chen [6], this curve shows a similar shape but not the identical damage sequence.

The cell structure tested can be described by Fig. 5. Through the rupture process of the cell package, it is clearly visible that at least four polymer-based encapsulation layers have been adopted for fabricating this Konarka OPV module. According to the stress–strain curve we obtained (Fig. 4), the first fall with approximately 35% strain is due to the rupture of internal encapsulation layer 2 (the layer in direct contact with electrode 2), together with the bottom encapsulation layer (external encapsulation layer 2 in Fig. 5). In most samples we tested, these two layers burst at the same time, which is likely due to the strong adhesion between them. We also once observed a separate rupture of the two layers, which proves that the cell adopts two different layers. Afterwards, near the strain of 65%, the cell shows the rupture of the top encapsulation layer (external encapsulation layer 1 in Fig. 5). At the very end of the curve, near the strain of 68%, the cell shows the largest fall, corresponding to the rupture of internal encapsulation layer 1. The close distance of these two falls may imply that these two layers adopt very similar materials. Later in this work, the electrical data prove that the two electrodes are damaged much earlier than the encapsulation layers' failure.

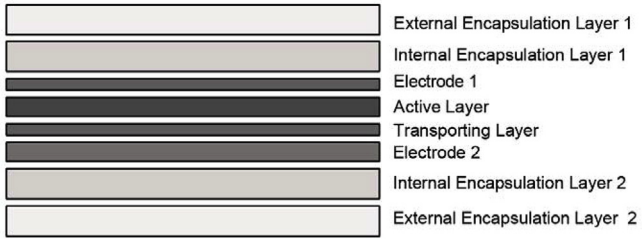

Fig. 5. Solar cell sample's layering structure.

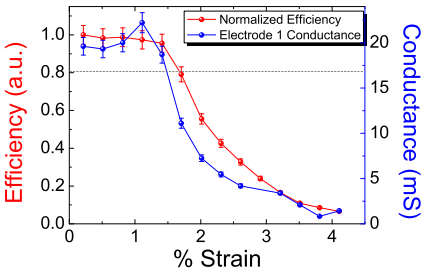

Fig. 6. Sample cell normalized efficiency and electrode 1 conductance through tensile test.

4.1.3. Electrical characterization

Fig. 6 illustrates how the cell efficiency and the conductance of electrode 1 (the transparent electrode) deteriorate with increasing strain of the whole cell package. It can be seen that after the cell reaches approximately 2% strain, it loses 50% of its initial efficiency. At strain of 3%, the cell has only 20% of its initial efficiency. The cell generates almost no power after the strain reaches 4% strain. From the figure, we can also see that the conductance of electrode 1 follows almost the same decreasing trend through the test. This implies that a highly likely reason for the cell efficiency degradation is the loss of electrode 1 conductance, which is later verified with the *I–V* curve. Considering the above two facts, if we assume that the critical point of the OPV stack refers to the moment when it loses 20% of its initial efficiency [32–34], which has been commonly used for defining the lifetime of photovoltaic devices, we can place the critical strain level of the cell at 1.8% and the corresponding critical stress at approximately 20 MPa. The fast degradation of the organic solar cells with strain critically underlines the importance of their mechanical properties for practical application as flexible PVs.

To investigate in detail which electrode is the main reason for the cell deterioration, we monitored the conductance of both electrodes through the tensile test. In Fig. 7, we can see that electrode 1 is much more sensitive to strain than electrode 2. With the strain at approximately 4–5%, where electrode 1 experiences a significant increase in resistance, the conductance of electrode 2 maintains its starting level. Actually, the resistance of electrode 2 starts to increase rapidly after the strain reaches 20%. With these results, we can conclude that the transparent electrode (electrode 1) used here is not mechanically robust upon large strain, whereas the metal electrode (electrode 2) is less sensitive to strain and could be a good choice with high stability for application in flexible BIPVs.

The influence of the increase in electrode resistance with increasing strain on the cell power conversion efficiency was also verified by the *I–V* curves as illustrated in Fig. 8. We can see that through the degradation of the cell, the decrease in I_{SC} (short-circuit current) plays a more important role than the decrease in V_{OC} (open-circuit voltage). Because the decrease in the short-circuit current is closely related to the increase in series resistance, we have a further confirmation of the main

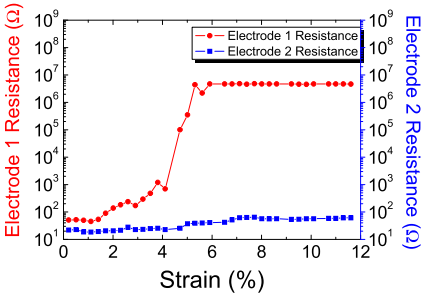

Fig. 7. Sample cell electrode 1 and electrode 2's conductance through tensile test.

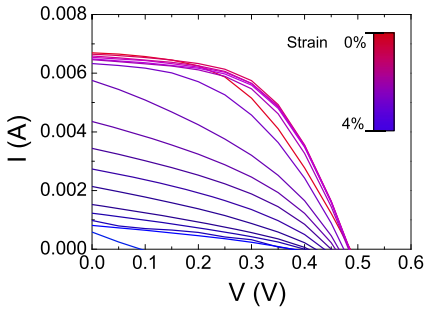

Fig. 8. I–V curve of tested cell sample from the strain of 0%–4%.

role played by electrode 1 in the degradation of the solar cell efficiency [32].

4.2. Characterization of architectural membrane printed OPV

4.2.1. Electrical characterization

Fig. 9a shows the recorded normalized conductance of Ag layers coated on PET and ETFE substrates through the uniaxial tensile tests. Both PET- and ETFE-printed specimens saw a rapid decrease in conductance during the initial phase, which implies that both of them are highly sensitive to tensile strains. However, the ETFE-based Ag layer experiences a slightly slower decrease in layer conductance at the same strain level compared with the PET-based one, especially within the 20–50% strain region, where the conductance–strain curve of ETFE printed specimen exhibits a lower line slope than PET printed one. This phenomenon reveals that the ETFE printed Ag layer conductance is still slightly less sensitive than the PET printed one with large strains, which is highly favoured for the utilization of ETFE as an OPV substrate.

Meanwhile, it can also be found that the ETFE-printed specimen saw a much higher strain at the rupture point, whereas the PET-based sample commonly met a brittle-like failure at a relatively smaller strain level. Moreover, at a higher strain level where the PET-printed specimen cannot reach, the ETFE-printed specimen's layer conductivity

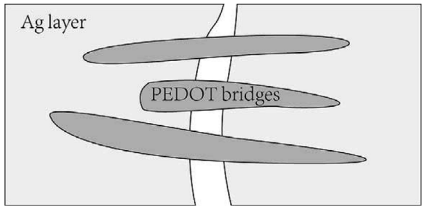

Fig. 10. "Bridging effect" of PEDOT layer over Ag layer through tensile test.

maintains its lower sensitivity to strains, decreasing gradually with stable speed until the final rupture.

The same phenomenon has also been observed with PEDOT/Ag layers coated on PET and ETFE substrates (Fig. 9b). It can be seen that the conductance–strain curves of PEDOT/Ag layers adopt quite similar shapes compared with those in Fig. 9a.

To further investigate the role of PEDOT in PEDOT/Ag layers, another set of tests has been performed with the same specimen form and experimental configuration.

Fig. 9c shows a clear difference between Ag/PET and PEDOT/Ag/PET configurations. At the same strain level, the PEDOT/Ag/PET configuration generally maintains higher conductance than the Ag/PET configuration. To reach 80% of the initial normalized conductance, the configuration with PEDOT as the top layer can withstand almost double strain compared with the Ag/PET-based one. This demonstrates that PEDOT helps increase the conductance of the Ag layer through the tensile stretching, especially after the specimen has reached the 10% strain level.

This phenomenon could be explained by the "bridging effect", as depicted in Fig. 10. Through the imposed tensile forces, the Ag layer will experience increasing strains all over the layer. Some high-strain locations will develop into cracks over the Ag layer, where the charge carrier mobility will be greatly reduced when applied in OPVs. However, the additional PEDOT layer above can partially ameliorate this phenomenon. Although the PEDOT layer will also develop cracks upon strains, the double-layer structure still maintains a certain probability of inter-crossing between the two layers. When this occurs over the

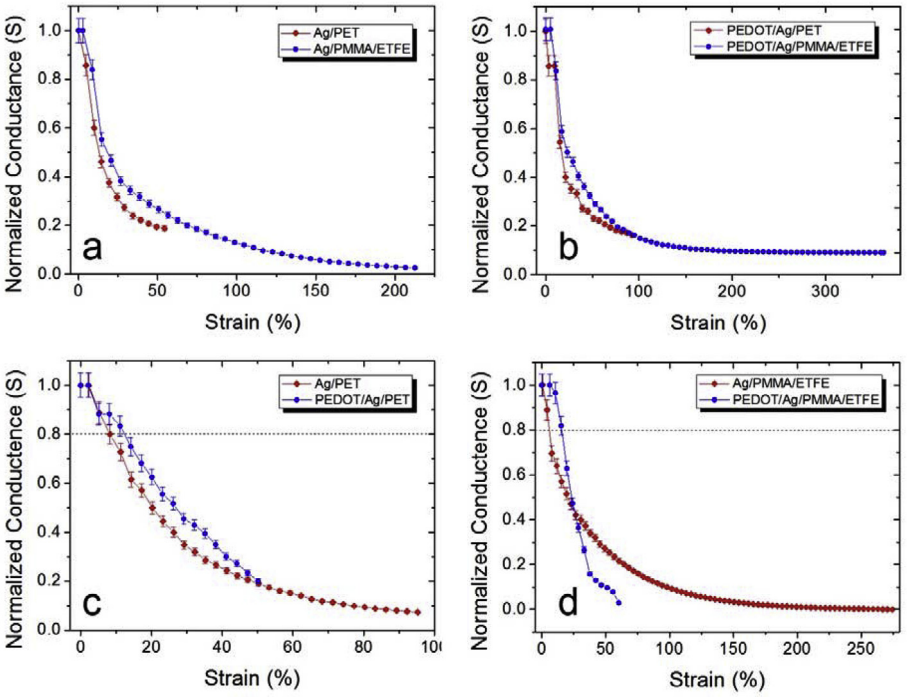

Fig. 9. Conductance through tensile test of specimen (a) Ag/PET & Ag/PMMA/ETFE; (b) PEDOT/Ag/PET & PEDOT/Ag/PMMA/ETFE; (c) Ag/PET & PEDOT/Ag/PET; (d) Ag/PMMA/ETFE & PEDOT/Ag/PMMA/ETFE.

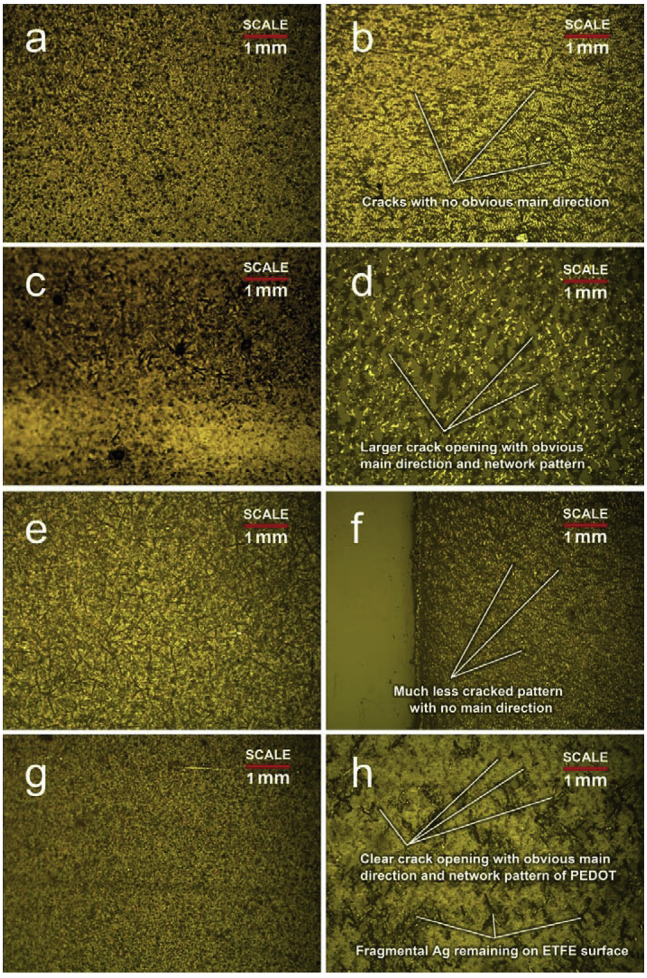

Fig. 11. Specimen observed under 10 × microscopes of (a) Ag/PET layer before tensile test; (b) stretched Ag/PET layer; (c) Ag/PMMA/ETFE layer before tensile test; (d) stretched Ag/PMMA/ETFE layer; (e) PEDOT/Ag/PET layer before tensile test; (f) stretched PEDOT/Ag/PET layer; (g) PEDOT/Ag/PMMA/ETFE layer before tensile test; (h) stretched PEDOT/Ag/PMMA/ETFE layer.

cracks of the Ag layer, the PEDOT can act as a bridge to increase the mobility of charge carriers through those cracks. Eventually, this will help ease the effect of the strain on the Ag layer conductance.

Through the results comparison of Ag/PMMA/ETFE and PEDOT/Ag/PMMA/ETFE configurations, as shown in Fig. 9d, we can find similar behaviour with a strain of less than 25%. The configuration with the PEDOT top layer maintains almost the same conductance level with double the strain of the Ag/PMMA/ETFE configuration. This could be explained similarly with the "bridge effect" from the PEDOT layer. However, with a strain higher than 25%, we observe a quite different phenomenon. In Fig. 9d, we can clearly observe crossing at the 25% strain of the Ag/PMMA/ETFE and PEDOT/Ag/PMMA/ETFE configuration curves. After 25% strain, the PEDOT/Ag/PMMA/ETFE specimen saw a more rapid decrease in conductance than the Ag/PMMA/ETFE specimen.

4.2.2. Morphology characterization

The stretched samples with different configurations were then observed under the microscope as shown in Fig. 11–12.

Fig. 11a–b shows the texture of the Ag/PET layer before and after the tensile test. Small cracks with no obvious main direction were scattered over the PET substrate. Compared with Fig. 11c–d of Ag/ETFE specimens, where the rupture occurs with a much larger strain and the printed Ag layer sees larger crack openings, the PET substrate acts as

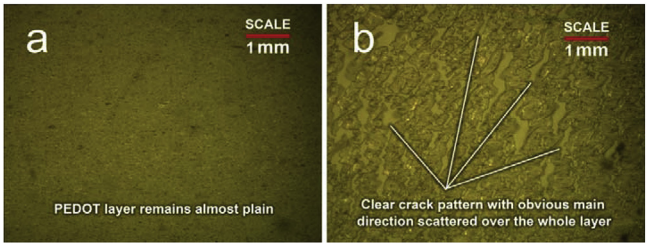

Fig. 12. Specimen observed under 10 × microscopes of (a) PEDOT/PET layer after tensile test (b) PEDOT/PMMA/ETFE layer after tensile test.

the bottleneck of the printed electrode layer. The crack pattern on ETFE also sees a more obvious main direction perpendicular to the stretching direction, which is probably the reason for the lower sensitivity of the ETFE printed Ag layer to strain because the resulting network pattern of the Ag layer can be more beneficial to the layer conductance than the orderless crack pattern on PET.

A similar situation has been observed with PEDOT/Ag/PET and PEDOT/Ag/PMMA/ETFE configurations (Fig. 11e–h). The PET-based specimen sees a much less cracked pattern compared with the ETFE-based specimen.

However, in contrast to the PET-based configuration, the PEDOT/Ag/PMMA/ETFE specimen sees much less Ag remaining on the ETFE surface after the tensile test compared with the Ag/PMMA/ETFE configuration. This can explain why in Fig. 11g–h, with strain larger than 25%, the PEDOT/Ag/PMMA/ETFE specimen met a more rapid conductance decrease. In Fig. 11h, we can also observe the smaller cracks of the PEDOT layer compared with the fragmental Ag shards below it. This also proves our "bridging effect" assumption of the PEDOT layer.

In Fig. 12, we also reported the texture of the PEDOT/PET and PEDOT/PMMA/ETFE layer after the tensile test. Because the PET layer ruptures at a relatively lower strain, the PET printed PEDOT layer remains almost plain, whereas the ETFE printed PEDOT layer shows an obvious crack pattern. The crack pattern shows a scattered distribution over the whole layer and also a more obvious main direction perpendicular to the stretching direction, quite similar to that seen with the Ag layer in the stretched Ag/PMMA/ETFE specimen.

However, the crack openings are still not comparable with those of the Ag layer in the PEDOT/Ag/PMMA/ETFE configuration. This further confirms the PEDOT layer's bridging effect.

5. Conclusions

This work proposed a coupled mechanical and electrical characterization method to monitor the correlation of OPV electrode resistance and cell performance upon tensile strain and to verify the deterioration effect and reason for the tension strain on the OPV performance response.

The employment of the test method with a commercial OPV module implies the following.

First, the strength of the encapsulation layers, rather than the functional layer, is the decisive factor in the cell package ultimate strength.

Second, the transparent electrode in the test commercial OPV module is more sensitive to strain than the metal electrode, and the decrease in the transparent electrode conductance has been determined to be responsible for the cell degradation upon tensile strain. The transparent electrode in the tested OPV is therefore not mechanically robust upon large strain, whereas the metal electrode characterized by high strain stability is a better choice for PV flexible product integration. The threshold of tensile strain for the tested OPV module to lose function has been recorded at 1.8%, with the corresponding critical stress at approximately 20 MPa.

The key weakness of the electrode in OPV upon tensile strain

inspired the following employment of the coupled test with ETFE- and PET-printed OPV layers. The experimental results indicate the following.

The electrode conductance of both the ETFE printed Ag and Ag/PEDOT is less sensitive than the PET printed one at small strains (< 50%), where the PET-printed configuration commonly shows a brittle-like failure, but ETFE shows a plastic-like stretching. At higher strain levels (> 50%) where the PET-printed specimen cannot reach, the ETFE-printed electrode conductivity maintains lower sensitivity to strains.

Further data analysis together with microscopic characterization confirms the following.

The network pattern of ETFE-printed electrodes contributes to the lower sensitivity of ETFE-printed electrodes upon tensile strain. The adoption of Ag/PEDOT layering can improve the tensile strain threshold to approximately double for maintaining 80% of the initial normalized layer conductance. The favour of PEDOT in increasing the Ag layer conductance is due to the "bridging effect". It loses its effectiveness only at strain levels higher than 25%, with a PEDOT/Ag/PMMA/ETFE configuration, where less Ag remains on the substrates after tension.

Our coupled test methodology and test results provided valuable information on the effect of tensile strain on the electrical performance of the OPV layer and module. It will contribute to subsequent building of product development towards OPV integration onto ETFE membrane. More efforts are needed to find stretchable alternatives for OPV integration in flexible PV products. Further investigation is also required to explore the properties of direct-printed full OPV on ETFE or other architectural membrane materials.

Acknowledgements

This work began thanks to the project SOFT (Smart, Organic, Flexible and Translucent)–PV: Creation of a Photovoltaic Organic Cell on Fluoropolymeric Substrate to Integrate into Smart Building Envelopes co-financed by the Cariplo Foundation in 2009. This work also owes great thanks to Paolo Beccarelli, Hend Mohamed Ibrahim, Stefano Perissinotto, and Guglielmo Lanzani for their collaboration. The authors express sincere thanks to Fondo Giovani Italy, which provided the scholarship for carrying on this research. Special thanks also go to OMET s.r.l, which provided co-financial support for this research.

Appendix A. Supplementary data

Supplementary data related to this article can be found at http://dx.doi.org/10.1016/j.compositesb.2018.04.007.

References

[1] Nielsen TD, Cruickshank C, Foged S, Thorsen J, Krebs FC. Business, market and intellectual property analysis of polymer solar cells. Sol Energy Mater Sol Cells 2010;94:1553–71.
[2] Krebs FC. Fabrication and processing of polymer solar cells: a review of printing and coating techniques. Sol Energy Mater Sol Cells 2009;93:394–412.
[3] Hermenau M, Schubert S, Klumbies H, Fahlteich J, Müller-Meskamp L, Leo K, Riede M. The effect of barrier performance on the lifetime of small-molecule organic solar cells. Sol Energy Mater Sol Cell 2011;97:102–8. http://dx.doi.org/10.1016/j.solmat.2011.09.026.
[4] Galliot C, Luchsinger RH. Uniaxial and biaxial mechanical properties of ETFE foils. Polym Test 2011;30:356–65.
[5] Cremers J. Soft skins – innovative foil and textile architecture. Proceedings of IXth international scientific conference "new building technologies and design problems". Cracow, Poland: Technical University of Cracow; 2011. I, pp. 21–29.
[6] Chen X, Liu S. Mechanical testing and analysis of polymer based flexible solar cell and full cell packaging. 12th international conference on electronic packaging technology and high density packaging (ICEPT-HDP). IEEE; 2011. 978-1-4577-1769-7/11.
[7] Chen X, Wang S, Luo Z, Zhang S, Lv Z, Jiang H, Liu S. An investigation on structure and materials of laminated organic solar cell packaging. Electronic components and technology conference (ECTC) 62nd. IEEE; 2012. 978-1-4673-1965-2/12.
[8] Brand V, Levi K, McGehee MD, Dauskardt RH. Film stresses and electrode buckling in organic solar cells. Sol Energy Mater Sol Cells 2012;103:80–5.
[9] Cairns DR, Witte II RP, Sparacin DK, Sachsman SM, Paine DC, Crawford GP, Newton RR. Strain-dependent electrical resistance of tin-doped indium oxide on polymer substrates. Appl Phys Lett 2000;76:1425.
[10] Lipomi DJ, Tee BC-K, Vosgueritchian M, Bao Z. Stretchable organic solar cells. Adv Mater 2011;23:1771–5.
[11] Lipomi DJ, Lee JA, Vosgueritchian M, Tee BC-K, Bolander JA, Bao Z. Electronic properties of transparent conductive films of PEDOT: PSS on stretchable substrates. Chem Mater 2012;24:373–82.
[12] Lipomi DJ, Chong H, Vosgueritchian M, Mei J, Bao Z. Toward mechanically robust and intrinsically stretchable organic solar cells: evolution of photovoltaic properties with tensile strain. Sol Energy Mater Sol Cells 2012;107:355–65.
[13] Lipomi DJ, Bao Z. Stretchable, elastic materials and devices for solar energy conversion. Energy Environ Sci 2011;4:3314.
[14] Benight SJ, Wang C, Tok JBH, Bao Z. Stretchable and self-healing polymers and devices for electronic skin. Prog Polym Sci 2013;38:1961–77.
[15] Kaltenbrunner M, White MS, Głowacki ED, Sekitani T, Someya T, Sariciftci NS, Bauer S. Ultrathin and lightweight organic solar cells with high flexibility. Nat Commun 2011;3:770.
[16] Leppänen K, Augustine B, Saarela J, Myllylä R, Fabritius T. Breaking mechanism of indium tin oxide and its effect on organic photovoltaic cells. Sol Energy Mater Sol Cells 2013;117:512–8.
[17] Cho C-K, Hwang W-J, Eun K, Choa S-H, Na S-I, Kim H-K. Mechanical flexibility of transparent PEDOT: PSS electrodes prepared by gravure printing for flexible or-ganic solar cells. Sol Energy Mater Sol Cells 2011;95:3269–75.
[18] Lim J-W, Cho D-Y, Eun K, Choa S-H, Na S-I, Kim J, Kim H-K. Mechanical integrity of flexible Ag nano wire network electrodes coated on colorless PI substrates for flexible organic solar cells. Sol Energy Mater Sol Cells 2012;105:69–76.
[19] Tait JG, Worfolk BJ, Maloney SA, Hauger TC, Elias AL, Buriak JM, Harris KD. Spray coated high-conductivity PEDOT: PSS transparent electrodes for stretchable and mechanically-robust organic solar cells. Sol Energy Mater Sol Cells 2013;110:98–106.
[20] Iwan A, Tazbir I, Sibiński M, Boharewicz B, Pasciak G, Schab-Balcerzak E. Optical, electrical and mechanical properties of indium tin oxide on polyethylene terephthalate substrates: application in bulk-heterojunction polymer solar cells. Mater Sci Semicond Process 2014;24:110–6.
[21] Savagatrup S, Printz AD, Wu H, Rajan KM, Sawyer EJ, Zaretski AV, Bettinger CJ, Lipomi DJ. Viability of stretchable poly(3-heptylthiophene) (P3HpT) for organic solar cells and field-effect transistors. Synth Met 2015;203:208–14.
[22] Sekine T, Ikeda H, Kosakai A, Fukuda K, Kumaki D, Tokito S. Improvement of mechanical durability on organic TFT with printed electrodes prepared from nanoparticle ink. Appl Surf Sci 2014;294:20–3.
[23] Yu Z, Niu X, Liu Z, Pei Q. Intrinsically stretchable polymer light-emitting devices using carbon nanotube-polymer composite electrodes. Adv Mater 2011;23:3989–94.
[24] Jones R., Johnson T., Jordan W., Wagner S., Yang J., Guha S.: Effects of mechanical strain on the performance of amorphous silicon triple-junction solar cells. Photovoltaic specialists conference, conference record of the twenty-ninth 2002 IEEE; (1214–1217) 0-7803-7471-1. doi: 10.1109/PVSC.2002.1190826.
[25] Gleskova H, Wagner S, Suo Z. a-Si:H thin film transistors after very high strain. J Non-Cryst Solids 2000;266–269:1320–4.
[26] Gleskova H, Wagner S, Soboyejo W, Suo Z. Electrical response of amorphous silicon thin-film transistors under mechanical strain. J Appl Phys 2002;92(10):6224–9.
[27] Gleskova H, Cheng I-C, Wagner S, Sturm JC, Suo Z. Mechanics of thin-film transistors and solar cells on flexible substrates. Sol Energy 2006;80:687–93.
[28] Antartis D, Chasiotis I. Residual stress and mechanical property measurements in amorphous Si photovoltaic thin films. Sol Energy 2014;105:694–704.
[29] Peters CH, Sachs-Quintana IT, Kastrop JP, Beaupré S, Leclerc M, McGehee MD. High efficiency polymer solar cells with long operating lifetimes. Adv Energy Mater 2011;1:491–4.
[30] Dupont SR, Oliver M, Krebs FC, Dauskardt RH. Interlayer adhesion in roll-to-roll processed flexible inverted polymer solar cells. Sol Energy Mater Sol Cells 2012;97:171–5.
[31] Corazza M, Rolston N, Dauskardt RH, Beliatis MJ, Krebs FC, Gevorgyan SA. Role of stress factors on the adhesion of interfaces in R2R fabricated organic photovoltaics. Adv Energy Mater June 8, 2016;6(11):1501927.
[32] Roth B, Savagatrup S, de los Santos NV, Hagemann O, Carlé JE, Helgesen M, Livi F, Bundgaard E, Søndergaard RR, Krebs FC, Lipomi DJ. Chem Mater 2016;28:2363–73.
[33] Krebs FC. Stability and degradation of organic and polymer solar cells. John Wiley & Sons; 2012.
[34] Grossiord N, Kroon JM, Andriessen R, Blom PWM. Degradation mechanisms in organic photovoltaic devices. Org Electron 2012;13:432–56.